

## Supplementary Materials

### **Novel Bi<sub>2</sub>S<sub>3</sub>/KTa<sub>0.75</sub>Nb<sub>0.25</sub>O<sub>3</sub> nanocomposite with high efficiency for photocatalytic and piezocatalytic N<sub>2</sub> fixation**

<sup>1</sup>Lu Chen <sup>a</sup>, <sup>1</sup>Xiaoquan Dai <sup>a</sup>, Xiaojing Li <sup>a</sup>, Junfeng Wang <sup>a</sup>, Huafong Chen <sup>a</sup>, Xin Hu <sup>b</sup>, Hongjun

Lin <sup>c</sup>, Yiming He <sup>a, b\*</sup>, Ying Wu <sup>b\*</sup>, Maohong Fan <sup>d, e\*</sup>

*<sup>a</sup>Department of Materials Science and Engineering, Zhejiang Normal University, Jinhua, 321004,*

*China*

*<sup>b</sup>Key Laboratory of the Ministry of Education for Advanced Catalysis Materials, Institute of*

*Physical Chemistry, Zhejiang Normal University, Jinhua, 321004, China*

*<sup>c</sup>College of Geography and Environmental Sciences, Zhejiang Normal University, Jinhua, 321004,*

*China*

*<sup>d</sup>Departments of Chemical and Petroleum Engineering, University of Wyoming, Laramie, WY*

*82071, USA*

*<sup>e</sup>School of Energy Resources, University of Wyoming, Laramie, WY 82071, USA*

Corresponding author:

E-mail: [hym@zjnu.cn](mailto:hym@zjnu.cn) (Y. He); [yingwu@zjnu.cn](mailto:yingwu@zjnu.cn) (Y. Wu); [mfan@uwyo.edu](mailto:mfan@uwyo.edu) (M. Fan)

<sup>1</sup> These authors contribute equally.

### *1. Photo/piezocatalytic $N_2$ fixation reaction*

The photocatalytic  $N_2$  fixation of the synthesized  $Bi_2S_3/KTa_{0.75}Nb_{0.25}O_3$  (KTN) composite was performed under simulated sunlight irradiation. Before light irradiation, 50 mg of solid catalyst was added into a 100 mL methanol solution (containing 5 mL methanol and 95 mL deionized water) and stirred for 1 h in the dark to ensure an adsorption–desorption equilibrium. A 300W Xe lamp (PLS-SXE300, Beijing PefectLight) was used as a simulated sunlight source. The light intensity at the position of reactor is about 54 mW/cm<sup>2</sup>. At every one-hour intervals of irradiation, 3 mL suspension was collected and centrifuged to obtain liquid samples.  $NH_4^+$  concentration analysis was conducted using Nessler's reagent method, at  $\lambda=420$  nm in a UV-vis spectrophotometer. The photocatalytic  $N_2$  fixation in the presence of different scavengers was performed in a similar way. Only the scavenger is changed. For the reaction in the presence of  $N_2$ , the bubbling  $N_2$  (99.999%) flow rate was controlled to 50 mL/min. For the reaction under vacuum, the reactor was replaced with a closed quartz reactor. After the reaction solution and catalyst were added, the air in the reactor is evacuated. The relative pressure to the outside world is -97kPa (the real pressure is about 4.3 kPa).

The piezocatalytic  $N_2$  fixation was performed in a similar process. The catalyst amount is 50 mg, and the reaction solution is methanol solution (5 mL methanol and 95 mL deionized water). After stirred in the dark for 1 h, the solution was placed in the center of vibration source (an ultrasonic vibration machine, 60W, 40 kHz) to receive a continuous ultrasonic vibration bath. At regular intervals, 3 mL of suspension was taken out and tested using the Nessler's method.

### *2. Determination of $NH_3$ content by the NMR method*

After photocatalytic reaction for 5 hours, the obtained  $NH_4^+$  content was also

quantitatively determined by  $^1\text{H}$  nuclear magnetic resonance (NMR, 600 MHz, Bruker AV600) with external standards, which takes maleic acid ( $\text{C}_4\text{H}_4\text{O}_4$ ) as a reference. The calibration curve was created as follows. First, a series of  $\text{NH}_4^+$  solutions with known concentration were prepared in 0.01 M HCl as standards; second, 24.5 mL of the  $\text{NH}_4^+$  standard solution was mixed with 0.5 mL maleic acid (25  $\mu\text{g/mL}$ ); third, the mixture was concentrated to approximately 1 mL and then identified using  $^1\text{H}$  NMR spectroscopy (50  $\mu\text{L}$  deuterium oxide ( $\text{D}_2\text{O}$ ) was added in 0.45 mL concentrated solution before NMR detection); fourth, the calibration was achieved using the peak area ratio between  $\text{NH}_4^+$  and tris-maleate because the  $\text{NH}_4^+$  concentration and the area ratio are positively correlated. Similarly, the  $\text{NH}_4^+$  concentration after photocatalytic reaction was quantitatively determined by this method.

### 3. Characterizations of $\text{Bi}_2\text{S}_3/\text{KTN}$ photocatalysts

The Bi content in the  $\text{Bi}_2\text{S}_3/\text{KTN}$  composite was analyzed by inductively coupled plasma-optical emission spectrometer (ICP-OES) (Thermo Scientific, iCAP 7400). The K, Ta, and Nb content of  $\text{KTa}_{0.75}\text{Nb}_{0.25}\text{O}_3$  solid solution was analyzed via X Ray Fluorescence (XRF, Bruker S8 LION). X-ray diffraction (XRD) analysis was performed on a D8 Advance (Bruker AXS GMBH, Germany) X-ray diffractometer using  $\text{Cu K}\alpha$  radiation (40 kV/40 mA). The Raman spectra of the  $\text{Bi}_2\text{S}_3/\text{KTN}$  catalysts were recorded on a RM1000 spectrometer (Renishaw) via an excitation source of an Ar ion laser (514.5 nm). Scanning electron microscopy (SEM) was carried out on a Field emission scanning electron microscope (Hitachi S-4800) with the accelerating voltage of 5 kV. Transmission electron microscopy (TEM) was employed on a JEM-2010F transmission electron microscope via the accelerating voltage of 200 kV. The X-ray photoelectron spectroscopy (XPS) spectra of the catalysts were obtained via using a Thermo Scientific ESCALAB 250Xi

Microprobe instrument using Al-K $\alpha$  as a ray source. The C 1s signal was adjusted in the location of 284.6 eV. UV-visible diffuse reflection spectroscopy (DRS) was actualized on a UV-visible spectrophotometer (Agilent Cary5000) and the reference sample was BaSO<sub>4</sub>. Brunner–Emmet–Teller (BET) surface area analysis was performed by N<sub>2</sub> adsorption at 77 K on a 3H-2000PS2 apparatus (Beishide Instrument).

A CHI 660E electrochemical workstation with a standard three-electrode cell was employed to perform the photocurrent (PC) responses, the electrochemical impedance spectroscopy (EIS), linear sweep voltammetry (LSV), and Mott-Schottky measurements. The test was operated at room temperature. The catalyst, Ag/AgCl (saturated KCl), and a Pt wire were used as the working electrode, the reference electrode, and the counter electrode, respectively. 200 mL Na<sub>2</sub>SO<sub>4</sub> (0.5 M) aqueous solution was used as the electrolyte. A 300 W Xe lamp was served as the light source in PC measurement.

The working electrode was prepared as follows. 50 mg of catalyst and 20  $\mu$ L of ethanol was mixed in a 1.5 mL centrifuge tube, and sonicated for 15 minutes. Then, 25  $\mu$ L of perfluorosulfonic acid was added and sonicated for another 15 minutes to make sure that the catalyst sample is evenly dispersed in the solution. The obtained mixture was evenly coated on the conductive surface of a conductive glass to form a small square of 1.0 cm  $\times$  1.0 cm. Finally, the electrode was dried at room temperature for 24 hours. For the LSV analysis in an N<sub>2</sub> and Ar saturated environment, carbon conductive adhesive was used during the preparation of working electrode to increase the adhesion of catalyst sample. The size of carbon conductive adhesive is 1.0 cm  $\times$  1.0 cm, while the catalyst sample is coated on the carbon conductive adhesive. During the LSV test, the scan rate is 0.01 V/s, the sample interval is 0.001 V, the quiet time is 2 second, and the

sensitivity is 0.001 A/V.

#### *4. The N<sub>2</sub> temperature programmed desorption (N<sub>2</sub>-TPD) experiment*

The N<sub>2</sub>-TPD experiment was performed in Micromeritics AutoChem II Chemisorption Analyzer. Typically, 100 mg of catalyst was placed in a quartz reactor and pretreated in a He (99.999%, 30 mL/min) atmosphere at 100°C for 60 minutes. After the temperature was cooled to 30°C, the sample was adsorbed with N<sub>2</sub> (99.999%, 30 mL/min) for 60 minutes, and then purged with He for another 60 minutes. After that, the sample was heated from 30°C to 650°C at a heating rate of 10°C/min.

#### *5. Calculation of the apparent quantum efficiency of Bi<sub>2</sub>S<sub>3</sub>/KTN photocatalysts*

The quantum efficiency of catalyst 0.25% Bi<sub>2</sub>S<sub>3</sub>/KTN can still be calculated according to the following method ( $\lambda$  was assumed to be 360 nm):

The NH<sub>4</sub><sup>+</sup> generation rate is determined to be 561.6  $\mu\text{mol}\cdot\text{L}^{-1}\cdot\text{g}^{-1}\cdot\text{h}^{-1}$ . The consumed electrons (N<sub>e</sub>) can be calculated as follows:

$$N_e = (6.02 \times 10^{23} \text{ electrons/mol}) \times (561.6 \times 10^{-6} \text{ mol/L} \times 0.1 \text{ L}) \times 3 \div 3600 = 2.817 \times 10^{16} \text{ electrons}\cdot\text{s}^{-1}\cdot\text{g}^{-1};$$

The diameter of the reactor is 6.5 cm. The surface area (S) that can be irradiated by light is estimated.

$$S = 3.14 \times (3.25 \text{ cm})^2 = 33.16 \text{ cm}^2;$$

Since the power density (P<sub>d</sub>) at the position of catalyst is measured to be 0.054 W/cm<sup>2</sup>, the total energy (E) shined over catalyst is estimated to be:

$$E = S \times P_d = 33.16 \times 0.054 = 1.79 \text{ W, or } 1.79 \text{ J/s.}$$

The energy of each photon is  $E_p = hf = (6.63 \times 10^{-34} \text{Js}) \times (3 \times 10^8 \text{m/s}) / (\lambda \times 10^{-9} \text{m})$

Since  $\lambda = 360 \text{ nm}$ ,  $E_p = 5.525 \times 10^{-19} \text{ J}$ .

The number ( $N_p$ ) of photons hitting on catalyst in each minute is:

$$N_p = E/E_p = 1.79 \div (5.525 \times 10^{-19}) = 3.24 \times 10^{20};$$

Quantum efficiency (g) under light with wavelength 400 nm is estimated to be:

$$g = N_e/N_p = 2.817 \times 10^{16} (\text{electrons/s}) / 3.24 \times 10^{20} (\text{photons/s}) = 8.7 \times 10^{-5} \approx 0.008\%$$

By the same way, the quantum efficiency of catalyst 0.25%  $\text{Bi}_2\text{S}_3/\text{KTN}$  under light with different wavelength can be calculated.

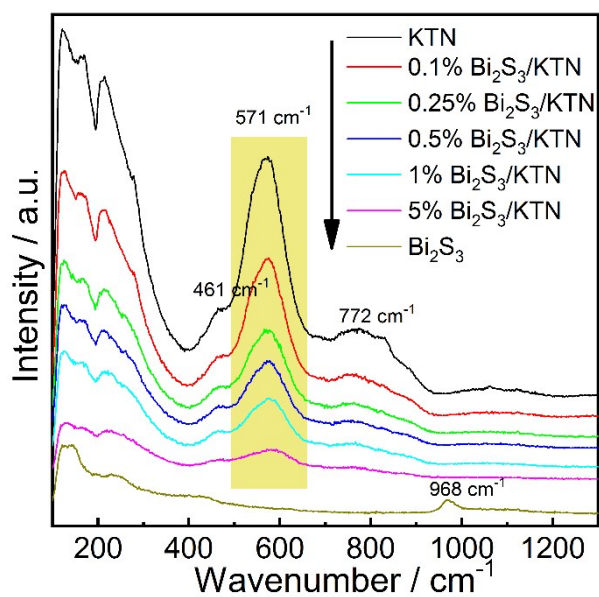


**Figure S1** Raman spectra of  $\text{Bi}_2\text{S}_3$ , KTN and  $\text{Bi}_2\text{S}_3/\text{KTN}$  composites

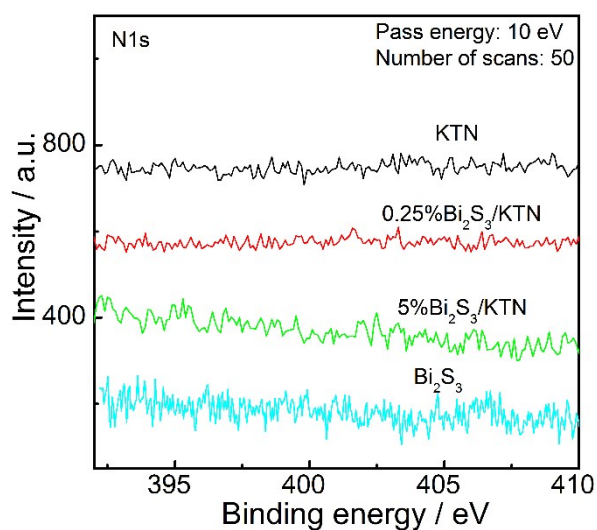


**Figure S2** N1s XPS spectra of  $\text{Bi}_2\text{S}_3$ , KTN and  $\text{Bi}_2\text{S}_3/\text{KTN}$  composites

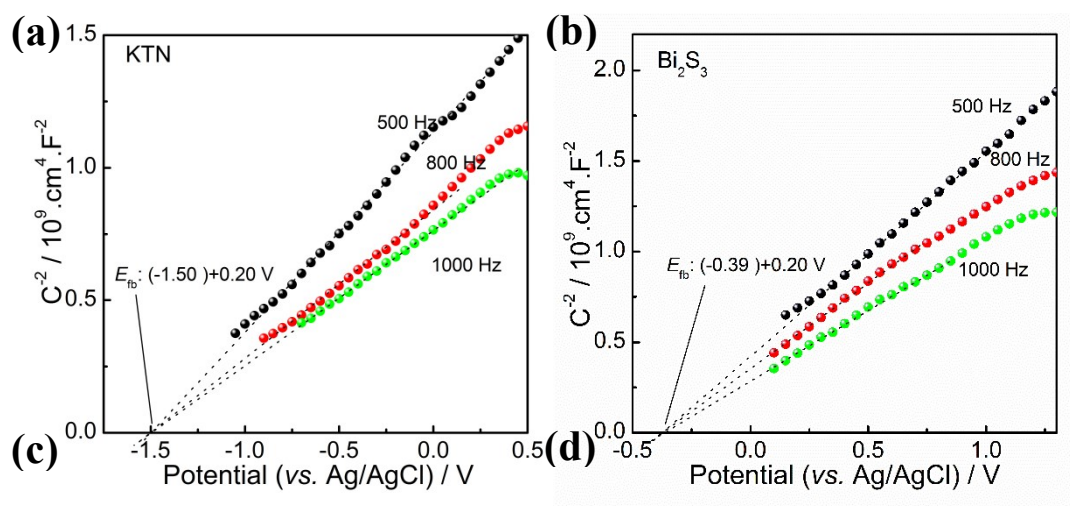


**Figure S3** Mott-Schottky plots of KTN (a) and  $\text{Bi}_2\text{S}_3$  (b).



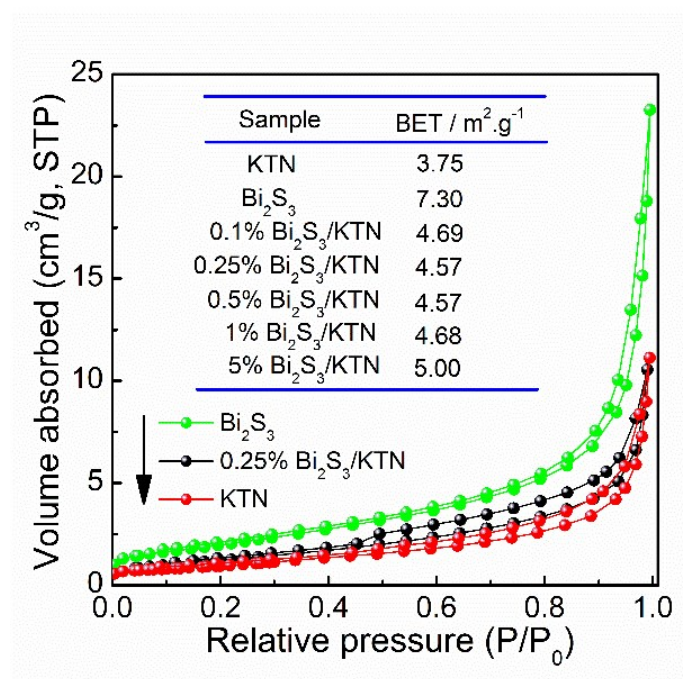


**Figure S4** N<sub>2</sub> adsorption-desorption isotherms of KTN, Bi<sub>2</sub>S<sub>3</sub> and 0.25%Bi<sub>2</sub>S<sub>3</sub>/KTN samples

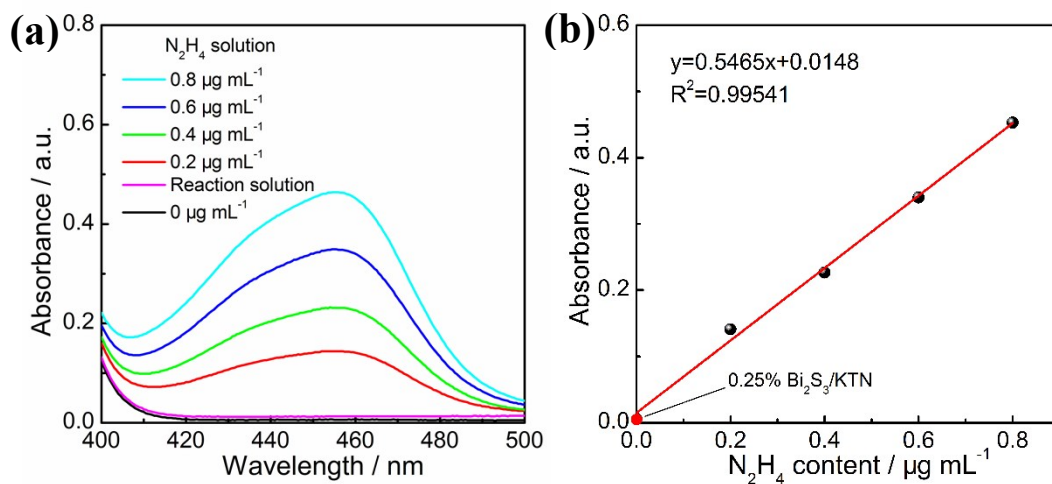


**Figure S5** UV-vis curves of various  $\text{N}_2\text{H}_4 \cdot \text{H}_2\text{O}$  concentrations after incubation for 15 min at room temperature and the (b) calibration curve used for the estimation of the  $\text{N}_2\text{H}_4 \cdot \text{H}_2\text{O}$  concentration

The concentration of  $\text{N}_2\text{H}_4$  was detected via the Watt and Chrisp method. Typically, 20  $\mu\text{L}$  of Ehrlich reagent (purchased from Sigma Aldrich) was added to 4 mL of a series of  $\text{N}_2\text{H}_4 \cdot \text{H}_2\text{O}$  standard solutions and the reacted solution. After incubation at room temperature for 15 minutes, the absorption spectra of the resulting solution were measured with a ultraviolet-visible (UV-vis) spectrophotometer. The formed complex was determined by absorbance at a wavelength of 455 nm.

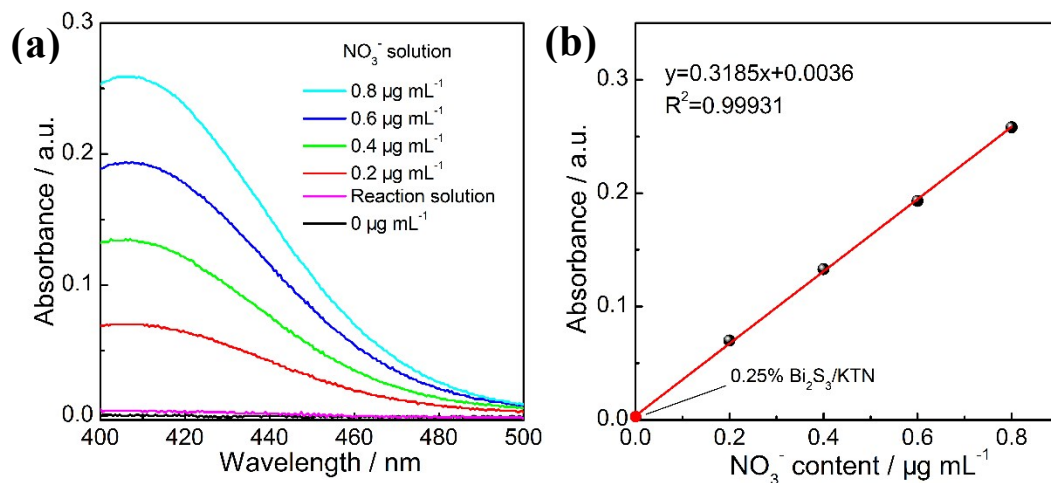


**Figure S6** UV-vis curves of various  $\text{NaNO}_3$  concentrations after incubation for 10 min at room temperature and the (b) calibration curve used for the estimation of the  $\text{NaNO}_3$  concentration

The  $\text{NO}_3^-$  in the solution was detected via the phenol disulfonic acid spectrophotometry. Typically, a series of 20mL  $\text{NaNO}_3$  standard solutions was prepared and the pH was adjusted to 9 with a NaOH solution. The solution was then heated to evaporate the water to dryness. After that, 0.5 mL of phenol disulfonic acid (AR, Sigma Aldrich) was added to dissolve the solid by stirring with a glass rod. After incubation at room temperature for 10 minutes, 5 mL of deionized water and 2 mL of ammonia were added. An ultraviolet-visible spectrophotometer was used to measure the absorbance of the resulting solution at a wavelength of 410 nm.

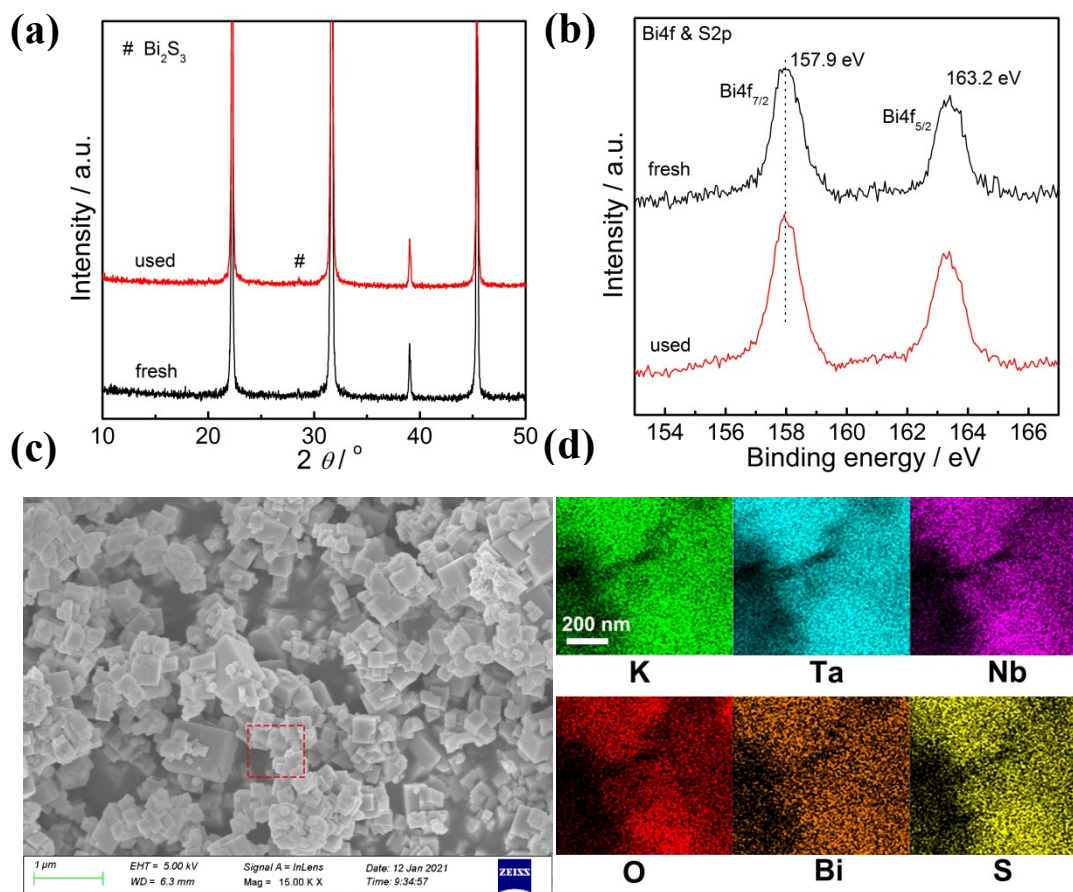


**Figure S7** XRD (a), XPS (b), SEM (c) and EDS mapping (d) of 0.25%Bi<sub>2</sub>S<sub>3</sub>/KTN after photocatalytic reaction.

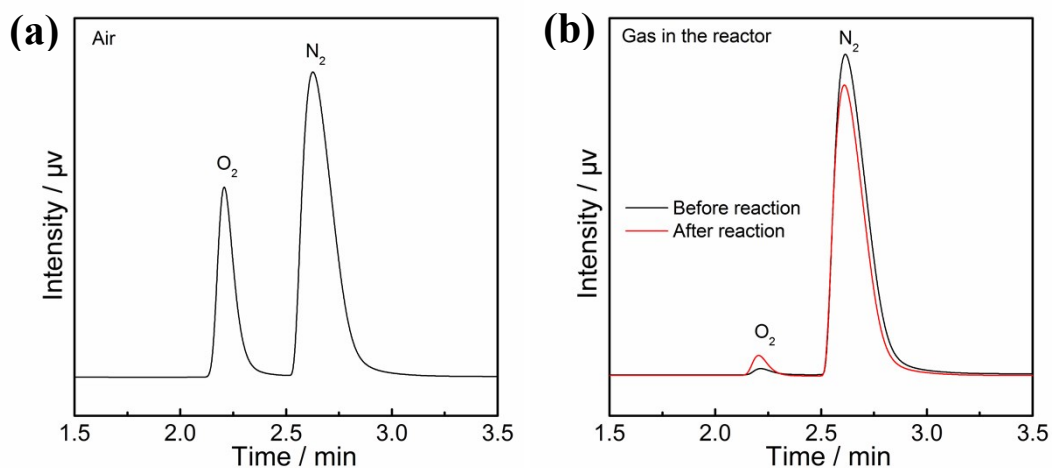


**Figure S8** GC profiles of air (a) and the reaction gas (b)

The photocatalytic  $N_2$  fixation with water as hole scavenger is performed in a closed reaction system. The amount of 0.25% $Bi_2S_3$ /KTN catalyst is 100 mg, and 200 mL deionized water is used as reaction solution. After the nitrogen (99.999%) has flowed into the reactor for 30 minutes, the reactor is sealed for the photocatalytic reaction. 5 mL of reaction gas was sampled and analyzed in a GC with a TCD detector before and after 5 hours reaction.

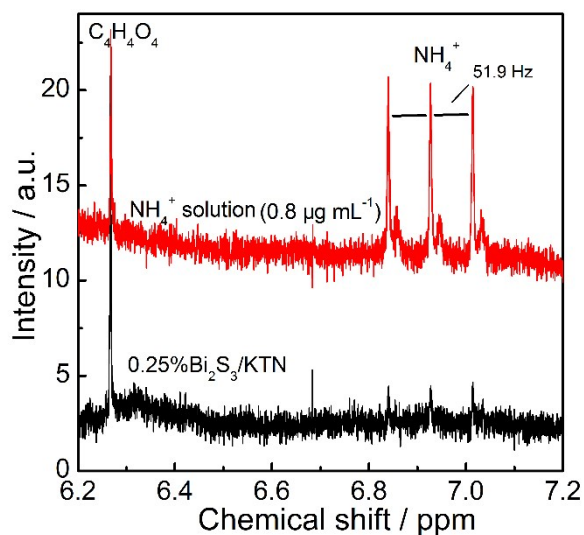


**Figure S9**  $^1\text{H}$  NMR spectrum of the solution after piezocatalytic  $\text{N}_2$  fixation reaction in the presence of  $0.25\%\text{Bi}_2\text{S}_3/\text{KTN}$ . (Notes: the reaction solution was 50 times concentrated.)

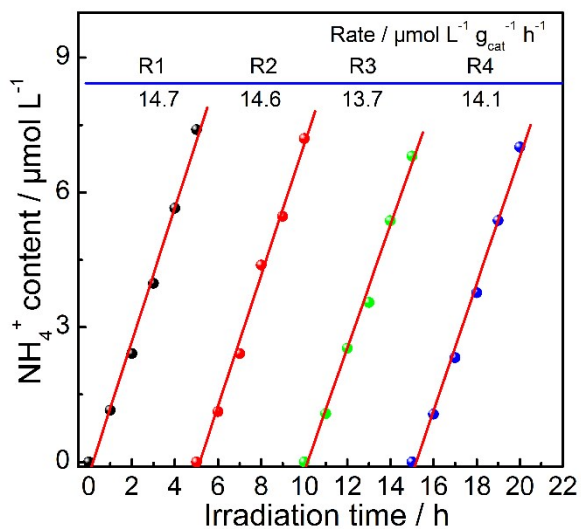


**Figure S10** The cycling test of  $0.25\%\text{Bi}_2\text{S}_3/\text{KTN}$  photocatalyst in piezocatalytic  $\text{N}_2$  fixation

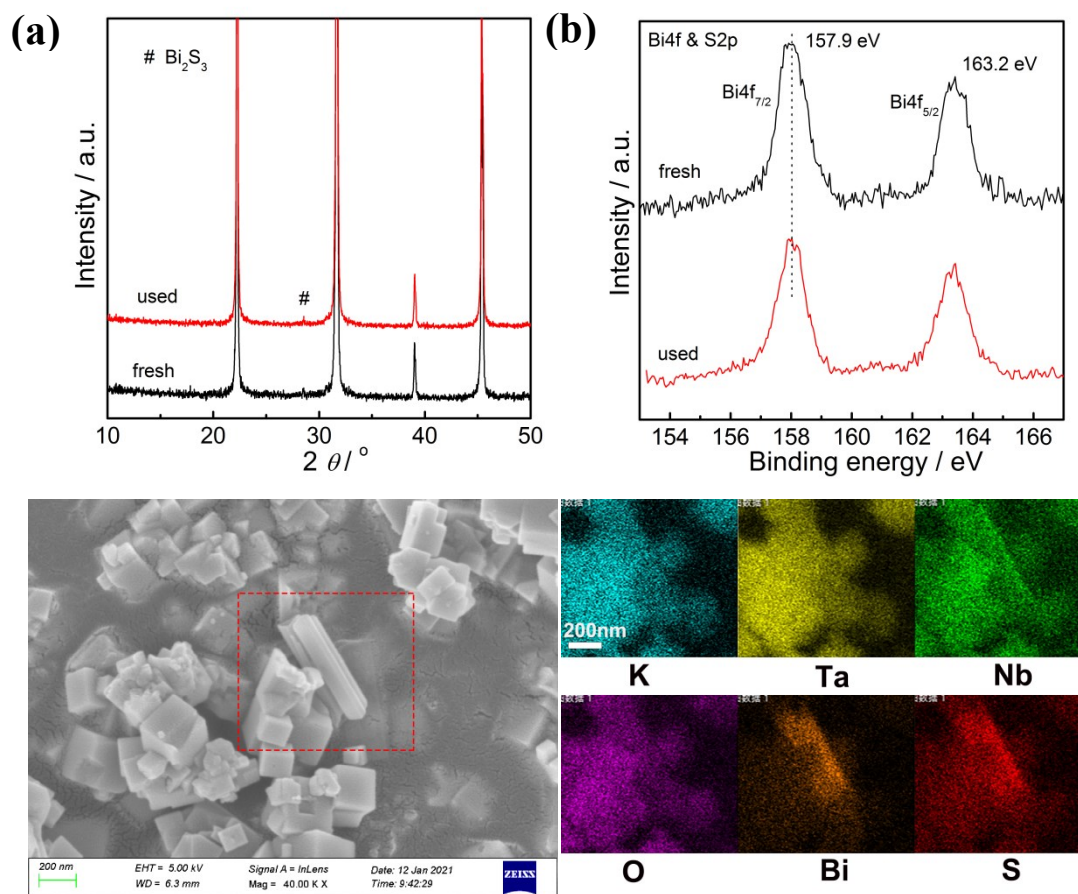


**Figure S11** XRD (a), XPS (b), SEM (c) and EDS mapping (d) of 0.25%Bi<sub>2</sub>S<sub>3</sub>/KTN after piezocatalytic reaction.

**Table S1** ICP results of Bi<sub>2</sub>S<sub>3</sub>/KTN composite photocatalysts with different amount of Bi<sub>2</sub>S<sub>3</sub>

Photocatalysts	Bi concentration /ppm		ICP Bi <sub>2</sub> S <sub>3</sub> content
	Theoretical result	ICP	
			result
0.1%Bi <sub>2</sub> S <sub>3</sub> /KTN	0.77	1.695	0.045
0.25%Bi <sub>2</sub> S <sub>3</sub> /KTN	2.553	4.225	0.151
0.5%Bi <sub>2</sub> S <sub>3</sub> /KTN	4.549	8.407	0.271
1%Bi <sub>2</sub> S <sub>3</sub> /KTN	12.209	16.642	0.734
5%Bi <sub>2</sub> S <sub>3</sub> /KTN	41.763	76.913	2.715

<sup>a</sup> 0.1g catalyst was dissolved in a certain amount of HNO<sub>3</sub> (2 M) solution for 1 hour. The obtained clear solution was then diluted into 100ml for ICP test.

**Table S2** Absolute electronegativity, estimated band gap, energy levels of calculated conduction band edge, and valence band at the point of zero charge for Bi<sub>2</sub>S<sub>3</sub> and KTN.

Semiconductors	Absolute electronegativity ( <i>X</i> )	Energy band gap <i>E<sub>g</sub></i> (eV)	Calculated conduction band edge (eV)	Calculated valence band edge (eV)
Bi <sub>2</sub> S <sub>3</sub>	5.5558	1.26	0.42	1.69
KTa <sub>0.75</sub> Nb <sub>0.25</sub> O <sub>3</sub>	5.3133	3.36	-0.86	2.50



**Table S3** Summary of reported photocatalysts for the N<sub>2</sub> reduction to NH<sub>3</sub>

Catalyst	Light	Nitrogen	Scavengers	NH <sub>3</sub>	generation	Ref.
	source	source		rate/ $\mu\text{mol}\cdot\text{L}^{-1}\cdot\text{g}^{-1}\cdot\text{h}^{-1}$		
Bi <sub>4</sub> O <sub>5</sub> Br <sub>2</sub> /ZIF-8	UV- vis	N <sub>2</sub>	water	327		[1]
SiO <sub>2</sub> /C-RP	UV- vis	N <sub>2</sub>	water	36.5		[2]
MoO <sub>3</sub> /BiOCl	UV- vis	N <sub>2</sub>	water	35.0		[3]
Ga <sub>2</sub> O <sub>3</sub> -DBD/g-C <sub>3</sub> N <sub>4</sub>	UV- vis	N <sub>2</sub>	ethanol	281		[4]
CeO <sub>2</sub> /BiFeO <sub>3</sub>	UV- vis	N <sub>2</sub>	water	117		[5]
FeS <sub>2</sub> /CeO <sub>2</sub>	UV- vis	N <sub>2</sub>	water	90.0		[6]
P25	UV- vis	N <sub>2</sub>	water	52.0		[7]
BiO quantum dots	UV- vis	N <sub>2</sub>	water	202		[8]
BiOCl	UV- vis	N <sub>2</sub>	methanol	68.9		[9]

$W_{18}O_{49}/g-C_3N_4$	UV- vis	$N_2$	ethanol	144	[10]
$Bi_2MoO_6/BiOBr$	UV- vis	$N_2$	water	90.7	[11]
$MoS_2/C/ZnO$	UV- vis	air	ethanol	245	[12]
$Ag/KNbO_3$	UV- vis	air	ethanol	385	[13]
$NiO/KNbO_3$	UV- vis	air	ethanol	470	[14]
$Bi_2S_3/KTN$	UV- vis	air	methanol	561	This work

**Table S4** Binding energies of all elements of 0.25% $Bi_2S_3/KTN$  photocatalysts before and after photocatalytic or piezocatalytic reaction.

Photocatalysts	Binding energy / eV					
	K2p <sub>3/2</sub>	Ta4f <sub>7/2</sub>	Nb3d <sub>5/2</sub>	O1s	Bi4f <sub>7/2</sub>	S2p <sub>3/2</sub>
Fresh	291.0	25.3	206.4	529.2	157.9	-
Photo-used	291.1	25.4	206.4	529.3	158.0	-

Piezo-used	291.0	25.3	206.5	529.3	158.0	-
------------	-------	------	-------	-------	-------	---

---

## References:

- [1] J.X. Liu, R. Li, X. Zu, X.C. Zhang, Y.F. Wang, Y.W. Wang, C.M. Fan, Photocatalytic conversion of nitrogen to ammonia with water on triphase interfaces of hydrophilic-hydrophobic composite  $\text{Bi}_4\text{O}_5\text{Br}_2/\text{ZIF-8}$ . *Chem. Eng. J.* 371 (2019) 796–803.
- [2] L. Lin, Q. Zhu, A. Cheng, L. Ma, Efficient solar-driven nitrogen fixation over an elemental phosphorus photocatalyst. *Catal. Sci. Technol.* 10 (2020) 4119–4125.
- [3] C.L. Xiao, H.P. Wang, L. Zhang, S.M. Sun, W.Z. Wang, Enhanced photocatalytic nitrogen fixation on  $\text{MoO}_2/\text{BiOCl}$  composite. *ChemCatChem* 11 (2019) 6467–6472
- [4] S. Cao, N. Zhou, F. Gao, H. Chen, F. Jiang, All-solid-state Z-scheme 3,4-dihydroxybenzaldehyde-functionalized  $\text{Ga}_2\text{O}_3/\text{graphitic carbon nitride}$  photocatalyst with aromatic rings as electron mediators for visible-light photocatalytic nitrogen fixation. *Appl. Catal. B: Environ.* 218 (2017) 600–610.
- [5] S. Mansingh, S. Sultana, R. Acharya, M.K. Ghosh, K.M. Parida, Efficient photon conversion via double charge dynamics  $\text{CeO}_2\text{-BiFeO}_3$  p-n heterojunction photocatalyst promising toward  $\text{N}_2$  fixation and phenol-Cr(VI) detoxification. *Inorg. Chem.* 59 (2020) 3856–3873.
- [6] S. Sultana, S. Mansingh, K. M. Parida, Phosphide protected  $\text{FeS}_2$  anchored oxygen defect oriented  $\text{CeO}_2\text{NS}$  based ternary hybrid for electrocatalytic and photocatalytic  $\text{N}_2$  reduction to  $\text{NH}_3$ . *J. Mater. Chem. A* 7 (2019) 9145–9153

- [7] Y. Liao, J.N. Lin, B.H. Cui, G. Xie, Well-dispersed ultrasmall ruthenium on TiO<sub>2</sub>(P25) for effective photocatalytic N<sub>2</sub> fixation in ambient condition. *J. Photochem. Photobiol. A: Chem.* 387 (2020) 112100.
- [8] S. Sun, Q. An, W. Wang, L. Zhang, J. Liu, W.A. Goddard Iii, Efficient photocatalytic reduction of dinitrogen to ammonia on bismuth monoxide quantum dots. *J. Mater. Chem. A* 5 (2017) 201–209.
- [9] H. Li, J. Shang, J. Shi, K. Zhao, L. Zhang, Facet-dependent solar ammonia synthesis of BiOCl nanosheets via a proton-assisted electron transfer pathway. *Nanoscale* 8 (2016) 1986–1993.
- [10] S. Hu, H. Zou, S.Z. Hu, Preparation of the W<sub>18</sub>O<sub>49</sub>/g-C<sub>3</sub>N<sub>4</sub> heterojunction catalyst with full-spectrum-driven photocatalytic N<sub>2</sub> photofixation ability from the UV to near infrared region. *New J. Chem.* 41 (2017) 8920–8926.
- [11] X.L. Xue, R.P. Chen, C.Z. Yan, Y. Hu, W.J. Zhang, S.Y. Yang, L.B. Ma, G.Y. Zhu, Z. Jin, Efficient photocatalytic nitrogen fixation under ambient conditions enabled by the heterojunctions of n-type Bi<sub>2</sub>MoO<sub>6</sub> and oxygen-vacancy-rich p-type BiOBr. *Nanoscale* 11 (2019) 10439–10444.
- [12] P.X. Xing, P.F. Chen, Z.Q. Chen, X. Hu, H.J. Lin, Y. Wu, L.H. Zhao, Y.M. He, Novel ternary MoS<sub>2</sub>/C-ZnO composite with efficient performance in photocatalytic NH<sub>3</sub> synthesis under simulated sunlight. *ACS Sustain. Chem. Eng.* 6 (2018) 14866–14879.
- [13] P.X. Xing, S.J. Wu, Y.J. Chen, P.F. Chen, X. Hu, H.J. Lin, L.H. Zhao, Y.M. He, New application and excellent performance of Ag/KNbO<sub>3</sub> nanocomposite in photocatalytic NH<sub>3</sub> synthesis. *ACS Sustain. Chem. Eng.* 7 (2019) 12408–12418.

- [14] P.X. Xing, W.Q. Zhang, L. Chen, X.Q. Dai, J.L. Zhang, L.H. Zhao, Y.M. He, Preparation of NiO/ $\text{KNbO}_3$  nanocomposite via photodeposition method and its superior performance in photocatalytic  $\text{N}_2$  fixation, *Sustain. Energy Fuels* 4 (2020) 1112–1117.